

Are the Hydrophobic AsPh_4^+ and BPh_4^- Ions Equally Solvated? A Theoretical Investigation in Aqueous and Nonaqueous Solutions Using Different Charge Distributions

Rachel Schurhammer and Georges Wipff*

Laboratoire MSM, UMR 7551, Institut de Chimie, Université Louis Pasteur, 4 rue Blaise Pascal, 67 000 Strasbourg, France

Received: April 25, 2000; In Final Form: July 18, 2000

We present a molecular dynamics study of the solvation properties of the tetrahedral AsPh_4^+ and BPh_4^- ions in water and chloroform solutions. According to the “extrathermodynamic” TATB (tetraphenylarsonium tetraphenylborate) hypothesis, these nearly isosteric ions have identical free energies of solvation in any solvent, as the latter are generally assumed to display little dependence on the details of the charge repartition, provided that the total \pm charge is delocalized and that the ion’s periphery is relatively inert. We compare eight different sets of charges obtained consistently for both ions and find that the anion is always better hydrated than the cation, as evidenced by ion–solvent interaction energies and changes in free energies of ion charging. This is explained by specific $\text{OH}-\pi$ bridging interactions in the anion and the positive electrostatic potential at the center of the fictitious AsPh_4^0 and BPh_4^0 all-neutral species. With all models, the cation is also predicted to be more easily transferred from water to dry chloroform. The conclusions obtained with standard solvent models (TIP3P water and OPLS chloroform) are validated by tests with the polarizable Wallqvist and Berne water model and the Chang et al. chloroform model, and with computer simulations on a “wet chloroform” solution. The recently developed TIP5P water model yields, however, much closer hydration energies of AsPh_4^+ and BPh_4^- . The importance of “long-range” electrostatic interactions on the charge discrimination by solvent is demonstrated by the comparison of standard vs corrected methods to calculate the Coulombic interactions. These results are important in the context of the “TATB hypothesis” and for our understanding of solvation of large hydrophobic ions in pure liquids or in heterogeneous liquid environments.

Introduction

The tetrahedral AsPh_4^+ and BPh_4^- ions play an important role in physical chemistry, as they are often used as reference states in solvation scales of individual ions.^{1–3} It is indeed generally assumed that the solvation properties of large hydrophobic ions are mostly determined by their size and the magnitude of their charge Q , but not by the \pm sign of Q . Thus, according to the extrathermodynamic TATB (tetraphenylarsonium tetraphenylborate) hypothesis, the nearly isosteric AsPh_4^+ and BPh_4^- ions are equally solvated in pure aqueous or in mixed water–liquid solvents, and have identical free energies of transfer from water to any solvent (s):

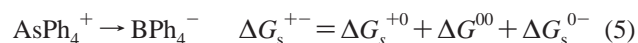
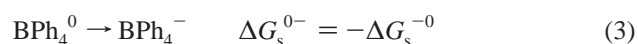
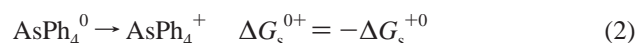
$$\Delta G_{\text{wat} \rightarrow s}(\text{AsPh}_4^+) = \Delta G_{\text{wat} \rightarrow s}(\text{BPh}_4^-) = \frac{1}{2} \Delta G_{\text{wat} \rightarrow s}(\text{AsPh}_4\text{BPh}_4) \quad (1)$$

On the basis of this hypothesis, the free energies of transfer of individual anions and cations from water to all kinds of solvents (polar/apolar, protic/aprotic, etc.) have been put on the same scale.³ Although free energies of solvation result from the interplay of solute–solvent and solvent–solvent interactions, including entropy and enthalpy components, most of the arguments in favor of the TATB hypothesis deal with the electrostatic solute–solvent interaction energy only. According to the continuum Born model, the excess free energy of solvation of a sphere of radius r and ionic charge Q , embedded in a continuum of dielectric constant ϵ , is $\Delta G_{\text{Born}} = (Q^2/2r)(1/\epsilon - 1)$,

* To whom correspondence should be addressed. E-mail: wipff@chimie.u-strasbg.fr.

and therefore independent of the sign of Q .⁴ As discussed by Marcus,⁵ the TATB hypothesis depends on the expectations that the interactions of the cation and anion with their solvent environments “should be independent of the sign of the charge, provided that these ions meet certain criteria: they should (i) have unit charge, (ii) be similar in most respects, (iii) have the same size, (iv) be very large, (v) be as nearly spherical as possible and (vi) have an inert periphery”.

This hypothesis represents a challenge for computer simulations. On the basis of free energy perturbation simulations with explicit representations of the ionic solutes and the solvents, it is possible to calculate the free energies of charging the neutral fictitious AsPh_4^0 and BPh_4^0 solutes (with all atomic charges imposed to be zero) to their charged AsPh_4^+ or BPh_4^- counterparts:



According to the TATB hypothesis, ΔG^{0+} should be equal to ΔG^{0-} in any solvent. Thus, the ΔG_s^{+-} free energy, which corresponds to the mutation of AsPh_4^+ to BPh_4^- should be zero in any solvent. These two ions should also have the same energy of transfer from water to any solvent. We recently reported molecular dynamics (MD) and free energy perturbation (FEP) results on AsPh_4^+ and BPh_4^- in water, chloroform, and

acetonitrile.⁶ It was found that the solvation of these ions and their free energies of transfer are very different, in contradiction with the TATB hypothesis. Other calculations on large spherical species S^+ and S^- of identical radii which meet the above criteria i–vi led also to the conclusion that the sign of the charge greatly determines the solvation and transfer properties of these ions, again in contradiction with the TATB hypothesis. These simulations⁶ used a standard methodology (residue-based cutoff) to calculate the nonbonded electrostatic and van der Waals energies and only one charge distribution on $AsPh_4^+$ and BPh_4^- . As similar energies were obtained with different cutoff distances, we concluded that the differentiation between the cation and the anion resulted mostly from short-range interactions and specific solvation patterns. As the treatment of boundaries may introduce deleterious artifacts,^{7–11} we more recently reinvestigated the S^0 , S^- , and S^+ spherical species in solution, using improved treatments of electrostatics:¹² the reaction field (RF), the particle mesh Ewald (PME), and the residue-based cutoff based on the “M3 point” defined in refs 7 and 11. It was found that the treatment of boundaries and “long-range” interactions play a major role in the \pm sign discrimination. With the RF-, PME-, or M3-based methods, the S^- anion was found to be better hydrated than S^+ , whereas S^+ was better solvated in chloroform and acetonitrile solutions.

In this paper we report recent investigations on $AsPh_4^+$ and BPh_4^- ions, with a main focus on their solvation properties as a function of the details of charge distribution. We compare eight sets (*set1* to *set8*) of atomic charges on each ion and calculate the corresponding solvation patterns and energies in TIP3P water and OPLS chloroform. Five sets have been fitted from the quantum mechanically calculated electrostatic potentials, using different basis sets and fitting procedures, while three other sets correspond to “handmade” models. As previous studies demonstrated that the largest differences in solvation energies ΔG^{+-} are observed in the aqueous phase,^{6,12} most of the simulations deal with water as solvent. We want to determine the role of charge distribution of a given ion and how the two ions compare with a consistent methodology in a given solvent model. One important issue is whether one of these electrostatic representations will lead to similar solvation properties of $AsPh_4^+$ and BPh_4^- . Comparison of the results obtained on these tetrahedral ions to those obtained with spherical S^+ and S^- models will give insight into the effect of the ion’s shape on the consequences of charge reversal. Given the importance of treatment of electrostatics at the boundaries, we also compare results obtained with a standard cutoff, as used in AMBER, to those obtained with the RF correction. The choice of solvent model may also be important to possibly discriminate $AsPh_4^+$ from BPh_4^- . We therefore decided to repeat some simulations using other water and chloroform models, including an explicit polarization energy term, in conjunction with two “extreme” charge representations of $AsPh_4^+$ and BPh_4^- .

Methods

We used the modified AMBER5.0 software¹³ with the following representation of the potential energy:

$$U = \sum_{\text{bonds}} K_r (r - r_{\text{eq}})^2 + \sum_{\text{angles}} K_\theta (\theta - \theta_{\text{eq}})^2 + \sum_{\text{dihedrals}} \sum_n V_n (1 + \cos n\phi) + \sum_{i < j} \left(\frac{q_i q_j}{R_{ij}} - 2\epsilon_{ij} \left(\frac{R_{ij}^*}{R_{ij}} \right)^6 + \epsilon_{ij} \left(\frac{R_{ij}^*}{R_{ij}} \right)^{12} \right)$$

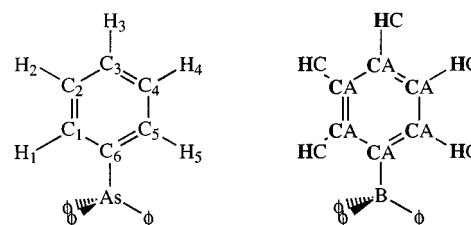


Figure 1. Atom labels (left) and AMBER atom types (right) used in both $AsPh_4^+$ and BPh_4^- ions.

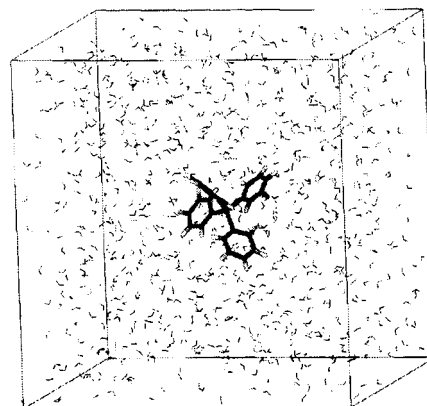


Figure 2. Simulation box: the $AsPh_4^+$ cation in water.

The parameters used to calculate U came from the AMBER force field.¹⁴ The atom types for $AsPh_4^+$ and BPh_4^- are given in Figure 1. The torsion around the B–C and As–C dihedrals was modeled with zero V_n terms, to allow for “free rotation”. Indeed, according to HF quantum mechanical calculations we performed with a 6-311G(df,p) basis set on Me_3B-Ph^- and Me_3As-Ph^+ (i.e., in the absence of steric phenyl–phenyl repulsions), the barriers are low (0.5 and 0.1 kcal/mol, respectively).¹⁵

Unless otherwise specified, the water and chloroform solvents were represented explicitly with the TIP3P¹⁶ and OPLS¹⁷ models, respectively. Some test simulations were repeated with the polarizable RER(pol) water model of Wallqvist and Berne (referred to later as WB)¹⁸ and with the all-atom polarizable chloroform model of Chang et al.,¹⁹ based on the methodology outlined in ref 20. The nonbonded interactions were calculated with a cutoff of 11 Å in water and 15 Å in chloroform. The solute, considered as a single residue, was immersed at the center of a cubic box. The water box was of 30 Å length and contained 873 water molecules, while the chloroform box was of 38 Å length and contained 390 solvent molecules, represented with periodic boundary conditions in the three directions (Figure 2).

The MD simulations were performed at 300 K, at $P = 1$ atm. All O–H, H···H, C–Cl, and Cl···Cl “bonds” were constrained with SHAKE, using a time step of 2 fs. After 1000 steps of energy minimization, each MD was run for 200 ps.

Long-Range Electrostatic Interactions. Long-range electrostatics contributes to the solvation energy of ionic species.²¹ As far as *differences* in solvation energies of like-charged solutes are concerned, these long-range energy contributions can generally be neglected. For ion charging processes, or for comparison of \pm charged solutes, the problem is more complex. With Ewald summation, the electrostatic interactions between the solute and the neutralizing background have the same magnitude for \pm charged solutes, and the *difference* in free energies of charging the cation/anion cancels out. An alternative and computer less demanding procedure is to use the RF correction for the electrostatics near the cutoff boundaries. We

TABLE 1: Atomic Charges on AsPh₄⁺ and BPh₄⁻ Obtained with Different Basis Sets and Fitting Procedures^a

ion	method	basis		X	C1/C5	C2/C4	C3	C6	H1/H5	H2/H4	H3
AsPh ₄ ⁺	ESP ^b	3-21G*	<i>set1</i>	0.76	-0.12	-0.16	-0.07	-0.12	0.15	0.18	0.15
		MK-ESP		3-21G*	-0.92	-0.27	-0.18	-0.09	0.47	0.22	0.19
	CHELP	6-311G*	<i>set2</i>	-0.86	-0.23	-0.19	-0.055	0.43	0.20	0.18	0.17
		6-311G(df,p)		-0.90	-0.24	-0.17	-0.06	0.455	0.19	0.18	0.16
		3-21G*	<i>set3</i>	1.12	0.01	-0.12	0.01	-0.25	0.03	0.14	0.09
		6-311G*		1.10	0.03	-0.13	0.035	-0.24	0.02	0.13	0.08
	CHELPG	6-311G(df,p)	<i>set4</i>	1.28	0.07	-0.17	0.11	-0.34	0.02	0.13	0.06
		3-21G*		-0.04	-0.10	-0.17	-0.05	0.12	0.12	0.17	0.15
	Mulliken	6-311G*	<i>set5</i>	-0.02	-0.10	-0.17	-0.05	0.115	0.12	0.16	0.15
		6-311G(df,p)		0.10	-0.05	-0.15	-0.01	0.065	0.08	0.14	0.13
		3-21G*	<i>set6</i>	1.44	-0.25	-0.23	-0.20	-0.33	0.28	0.28	0.29
		6-311G*		1.33	-0.22	-0.20	-0.19	-0.33	0.26	0.25	0.26
		6-311G(df,p)	<i>Handmade</i>	1.16	-0.13	-0.125	-0.11	-0.32	0.18	0.18	0.18
				0.5	0.011	0.011	0.011	0.011	0.011	0.011	0.011
				1.0	0.0	0.0	0.0	0.0	0.0	0.0	0.0
				0.024	0.022	0.022	0.022	0.022	0.022	0.023	0.022
BPh ₄ ⁻	ESP ^b	3-21G*	<i>set1</i>	-0.48	-0.29	-0.15	-0.24	0.30	0.14	0.13	0.15
		MK-ESP		3-21G*	-1.72	-0.36	-0.17	-0.25	0.69	0.19	0.14
	CHELP	6-311G*	<i>set2</i>	-1.51	-0.32	-0.17	-0.23	0.61	0.17	0.13	0.13
		6-311G(df,p)		-0.52	-0.30	-0.17	-0.23	0.63	0.16	0.12	0.11
		3-21G*	<i>set3</i>	0.12	-0.07	-0.10	-0.20	0.06	-0.02	0.08	0.08
		6-311G*		0.18	-0.02	-0.14	-0.125	0.02	-0.03	0.07	0.05
	CHELPG	6-311G(df,p)	<i>set4</i>	0.20	-0.01	-0.13	-0.11	0.01	-0.04	0.06	0.04
		3-21G*		-0.84	-0.21	-0.14	-0.22	0.39	0.08	0.11	0.11
	Mulliken	6-311G*	<i>set5</i>	-0.54	-0.15	-0.14	-0.19	0.285	0.05	0.09	0.09
		6-311G(df,p)		-0.52	-0.13	-0.13	-0.18	0.26	0.04	0.08	0.08
		3-21G*	<i>set6</i>	1.74	-0.29	-0.24	-0.265	-0.39	0.23	0.19	0.19
		6-311G*		1.08	-0.28	-0.21	-0.24	-0.27	0.22	0.18	0.17
		6-311G(df,p)	<i>Handmade</i>	1.22	-0.18	-0.13	-0.18	-0.36	0.15	0.10	0.105
				-0.5	-0.011	-0.011	-0.011	-0.011	-0.011	-0.011	-0.011
				1.0	0.0	0.0	0.0	0.0	0.0	0.0	0.0
				-0.024	-0.022	-0.022	-0.022	-0.022	-0.022	-0.023	-0.022

^a See Figure 1 for atom definitions. ^b Charges calculated with SPARTAN.²⁰

thus calculated the electrostatic interactions with an atom-based cutoff and the RF method, as described in ref 22. It considers a sphere of radius d_{cut} around the molecule, surrounded by a continuum medium of dielectric constant ϵ_s , polarized by the charges within the sphere. The interaction energy between the charge distribution inside the sphere and the polarized medium is calculated using the image charge method. With the RF method, the contribution of the peripheral solvent molecules to the electrostatic potential ϕ at the solute is zero. This is correct for neutral solutes (if d_{cut} is large enough), but not for charged ones, due to the nonrandom orientation of the solvent at the cutoff distance. However, the *difference* in $\phi(S^+)$ and $\phi(S^-)$ potentials is correctly accounted for.¹² On the basis of a comparison with Ewald results, we checked that this RF method correctly calculates the electrostatic potential ϕ at the center of a neutral sphere S^0 , as well as the *difference* $\Delta\phi$ in electrostatic potentials between $\phi(S^+)$ and $\phi(S^-)$ at the center of S^+ and S^- . Similarly, the *difference* in solvation free energies ΔG^{+-} of S^+ and S^- ions was found to be nearly identical with the RF and Ewald methods.¹²

For comparison, we also report some results of “standard calculations” which use a residue-based cutoff, where interactions between all atoms of molecules A and B (“residues”) are calculated if the distance between the corresponding “tested atoms” (O_{H2O} for water, C_{CHCl3} for chloroform, and any atom of the solute) is shorter than the d_{cut} distance.

Charge Fitting Procedures. Ab initio quantum mechanical calculations were performed at the Hartree–Fock level on AsPh₄⁺ and BPh₄⁻ with the Gaussian95 program²³ and the 3-21G*, 6-311G*, and 6-311G(df,p) basis sets. For each basis set, four sets of atomic charges were obtained using, respectively, the Mulliken partition scheme, the electrostatic potential fitting procedures of Merz–Kollman (MK-ESP), and the

CHELP and CHELPG procedures implemented in Gaussian95. Charges were calculated after 6-31G* energy minimization, starting from the X-ray structures of AsPh₄⁺ and BPh₄⁻. The optimized As–C (1.908 Å) and B–C (1.673 Å) distances are close to those in the crystal state (average values, retrieved from the Cambridge Crystallographic database,²⁴ are 1.91 and 1.66 Å, respectively). Another set of 3-21G* charges was derived from electrostatic potentials with the SPARTAN software.²⁵ Strictly speaking, these ions have no symmetry, but display pseudotetrahedral symmetry upon free rotation of the As–Ph and B–Ph bonds. The atomic charges were thus averaged on atom groups which become equivalent. The results are presented in Table 1.

Free Energy Calculations. The difference in free energies of solvation between two states was obtained using the statistical perturbation FEP theory and the windowing technique, with

$$\Delta G = \sum \Delta G_\lambda \quad \text{and} \quad \Delta G_\lambda = RT \text{Log} \left\langle \exp \frac{(U_\lambda - U_{\lambda+\Delta\lambda})}{RT} \right\rangle_\lambda$$

The potential energy U_λ was calculated using a linear combination of parameters (generally the charges) of the initial state ($\lambda = 1$) and final state ($\lambda = 0$): $q_\lambda = \lambda q_1 + (1 - \lambda)q_0$. The number of intermediate steps (“windows”) was 21 in water and 51 in chloroform. At each window, 2 ps of equilibration was followed by 3 ps of data collection, and the change of free energy ΔG_λ was averaged from the forward and backward cumulated values.

Analysis of Results. Average structures, radial distribution functions (RDFs), solute–solvent (E_{ss}) and solvent–solvent (E_{ss}) interaction energies and their electrostatic/van der Waals components were calculated from the trajectories saved every 0.5 ps.²⁶

The analysis of specific water hydrogen-bonding patterns to AsPh_4^+ and BPh_4^- was based on geometry considerations and used consistently for all systems. For each set of coordinates, we first selected all water molecules whose oxygen atom sits at less than 4.5 Å from the central atom X (As or B) and calculated the distances from the center of mass M_i of each phenyl ring i to H_{water} and O_{water} . The O–H π interactions were characterized by $\text{H}-M_i < 3 \text{ \AA} < \text{O}-M_i$. “Bridging” water was identified by two O–H π interactions per water molecule with two different rings. If one proton only was involved, the O–H π bond was “*exo*”. We checked on the graphics system that this procedure correctly selects the water molecules.

Results

Unless otherwise specified, all results correspond to the standard solvent models (TIP3P water and OPLS chloroform). We first describe the atomic charges obtained by the different models and the resulting solvation patterns and energies. The interaction energies in $\text{AsPh}_4^+ \cdots \text{H}_2\text{O}$ and $\text{BPh}_4^- \cdots \text{H}_2\text{O}$ supermolecules are compared from ab initio QM and molecular mechanics calculations. Finally, the differences in free energies of solvation between the two ions and in free energies of transfer from water to chloroform are assessed with the different models.

Charge Distributions in the AsPh_4^+ and BPh_4^- Ions. From the QM calculations, 13 different sets of atomic charges were derived for each ion. They are reported in Table 1, together with the three handmade models.

The first question concerns the q_X charge on the central atom. According to Pauling’s scale of electronegativities, both As ($\chi = 2.18$) and B ($\chi = 2.04$) are somewhat less electronegative than C ($\chi = 2.55$) and H ($\chi = 2.20$), and should be therefore somewhat more positively charged. Table 1 shows that this is not always the case as the charges are highly basis set and model dependent. For instance, q_{As} is negative ($-0.9 e$) with the MK-ESP model, but positive ($1.1-1.2 e$) with CHELP, and close to zero with CHELPG, while the Mulliken charges are the most positive ones ($1.1-1.4 e$). Similarly, the q_{B} charge ranges from -1.5 to $-1.7 e$ with MK-ESP, from -0.5 to -0.8 with CHELPG, from 0.1 to $0.2 e$ with CHELP, and from 1.1 to $1.7 e$ with Mulliken. Thus, *changes as a function of the fitting method are generally much larger than those due to the choice of basis set*. Similar changes are observed with the other atoms. For instance the q_{C6} charge on the *para* carbon ranges from -0.3 to $+0.4 e$ in AsPh_4^+ and from -0.4 to $+0.7 e$ in BPh_4^- . The aromatic protons are generally positively charged in both ions.

A second issue concerns the change in group polarities from AsPh_4^+ to BPh_4^- . For a given basis set and derivation method, there is no systematic sign inversion on the corresponding atoms of AsPh_4^+ and BPh_4^- (Table 1). Thus, *in no case does the sign inversion of the total charge correspond to an inversion of atomic charges*.

Because of computer time limitations, eight typical sets were selected to simulate AsPh_4^+ and BPh_4^- in solution. The selection was based on a “diversity” criterion, as some of them (e.g., those obtained with the 3-21G*, 6-311G*, and 6-311G(df,p) basis sets and the same fitting procedure) were quite similar. *Set1* to *set5* are QM derived charges (Table 1). Handmade models are *set6*, where the total charge is split on the central atom (50%) and on the four aryl groups (50%), *set7*, where the ± 1 charge is localized on the central atom only, and *set8*, where the ± 1 charge is equally distributed on all atoms. With these three models, the ions have an inert (*set7*) or nearly inert (*set6* and *set8*) periphery.

Ion Hydration and HO–H $\cdots\pi$ Interactions. The average structure of water around the central atom of the ions is characterized by the RDFs. They are represented in Figure 3 for the eight sets of charges. With most models, a clear difference is observed between the cation’s and anion’s hydration. At short distances ($< 5.0 \text{ \AA}$) the $\text{As}\cdots\text{H}_w$ and $\text{As}\cdots\text{O}_w$ curves for AsPh_4^+ are nearly superposed, as typically observed for spherical hydrophobic solutes, while for BPh_4^- the shortest $\text{B}\cdots\text{H}_w$ contacts are always shorter than the $\text{B}\cdots\text{O}_w$ ones. This is indicative of hydrogen-bonding interactions with BPh_4^- , which acts as a proton acceptor. Most of the anion’s and cation’s RDFs display a first peak at about 5 Å, which corresponds to solvent atoms sitting between phenyl rings, and a second one at about 8 Å, corresponding to the solvation of peripheral protons. There is thus no marked difference between the different models, except for *set5* (Mulliken charges) and *set7* (neutral aryl groups). In water, the phenyl groups of BPh_4^- do not rotate, while those of AsPh_4^+ undergo several rotations (see typical examples in Figure S1 in the Supporting Information). As such a difference in internal dynamics is also observed in the gas phase, it does not result from specific solvation effects.²⁷

A close look at the structures on the graphics system reveals typical “inner shell” hydrogen-bonding patterns (see Figure 4), where one O–H bond of water is nearly perpendicular to an aryl group. The geminal O–H bond is either turned *exo* (single OH– π interaction; Figure 4, left) or may also interact with the π system of the adjacent aryl group (bridging interaction). The two types of water molecules may be found simultaneously around BPh_4^- , while bridging water is never found around AsPh_4^+ . Figure 5 summarizes the results of a statistical analysis of OH– π interactions with the eight models and confirms the marked difference between AsPh_4^+ and BPh_4^- , as far as OH– π interactions are concerned. For the cation, with all models (except *set5*) non-hydrogen-bonded species are dominant, while the OH– π interactions are *exo* and involve one ring only. For the anion, the majority of configurations involve hydrogen-bonded water, with variable contributions of the monobridged and bisbridged arrangements. The latter are more important in the handmade than in the QM derived sets of charges. Due to specific interactions, reversing the total charge does not invert the first shell water dipoles. For BPh_4^- , π bridging water corresponds to the optimal orientation of the water dipole with respect to a negatively charged B center. Bridging water can further hydrogen bond to “second shell” water molecules. The expected inverted orientation around AsPh_4^+ is not observed, however, presumably because this would disrupt the connection with the second shell. Solvation of peripheral protons is more complex to analyze, as it is determined by the (generally weakly positive) charge of these atoms, as well as by interactions with the “inner shell” water molecules.

The polarizable WB water model has been tested in conjunction with the *set1* and *set8* representations of the ions. It leads to hydration patterns similar to those of the TIP3P water model. The RDFs are similar (Figure 3), although the O_w peak is more pronounced, and WB water makes somewhat closer contacts than does the TIP3P water. The statistical analysis of hydrogen-bonding patterns with WB water confirms that AsPh_4^+ forms only *exo* OH– π interactions, while BPh_4^- forms additional bridging hydrogen bonds in about 30% of the configurations (Figure 5).

The effect of ion charge on the solvation patterns can be seen in Figure 5, which shows that the all-neutral AsPh_4^0 and BPh_4^0 species display less OH– π interactions (about 15% with TIP3P

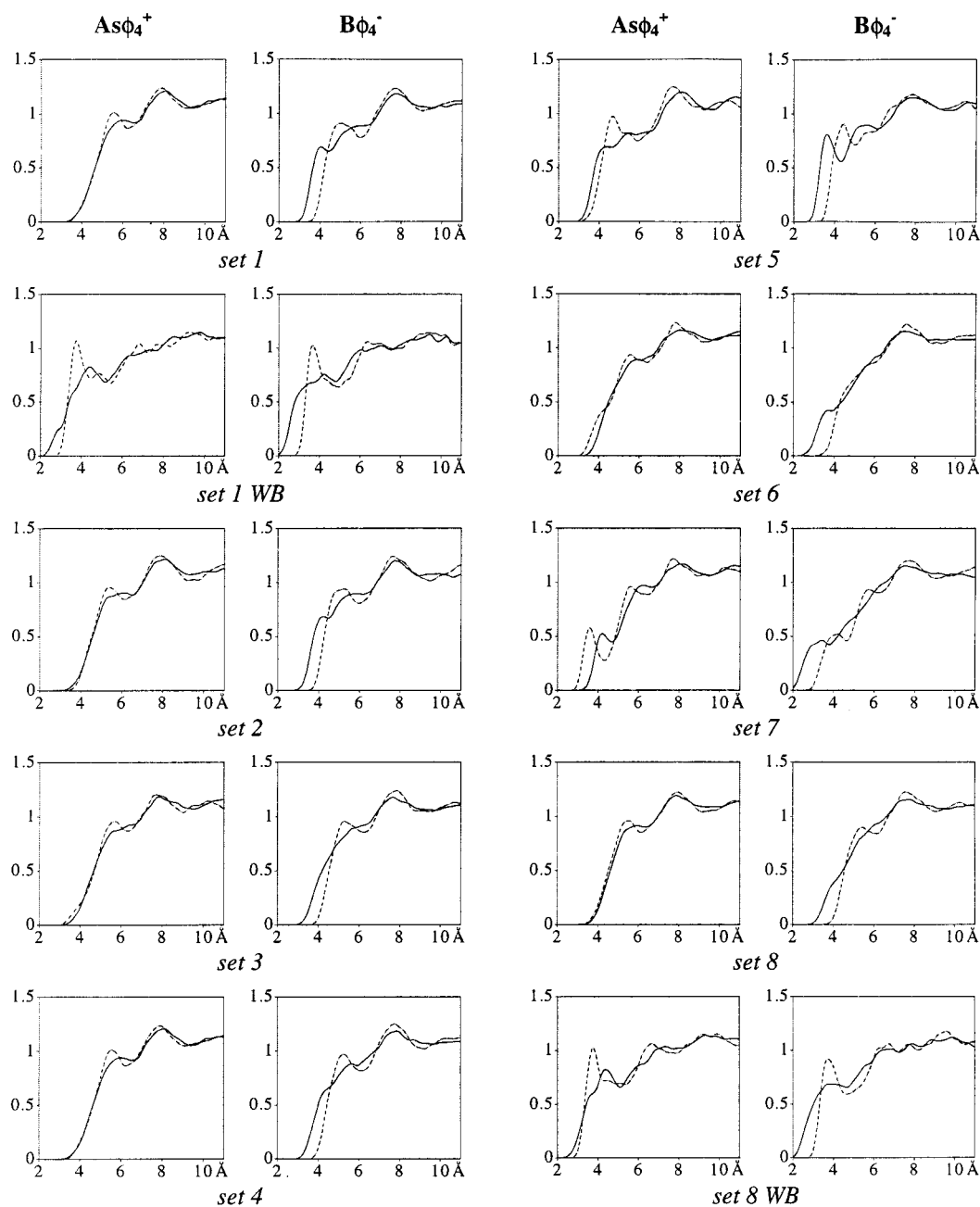


Figure 3. AsPh_4^+ , BPh_4^- ions in TIP3P water simulated with different charge distributions and 11 + RF conditions. RDFs around the central atom (As or B) of O_w (dotted line) and H_w (full line). The “WB” results are obtained with the polarizable water model of Wallqvist and Berne.¹⁸

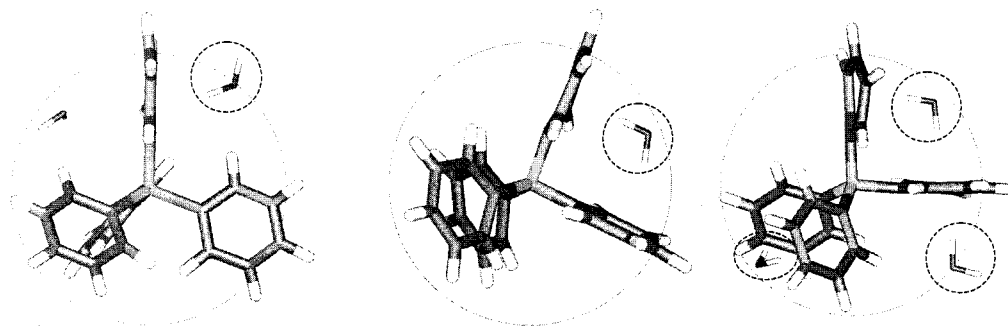


Figure 4. Typical positions of water molecules forming $\text{OH}-\pi$ interactions with AsPh_4^+ (left) and BPh_4^- (center and right).

water and 40% with WB water) than BPh_4^- but more than AsPh_4^+ .

$\text{AsPh}_4^+\cdots\text{H}_2\text{O}$ and $\text{BPh}_4^-\cdots\text{H}_2\text{O}$ Supermolecules. The importance of $\text{OH}-\pi$ interactions is further demonstrated by

exploratory QM calculations (3-21G* basis set) of the interaction energy ΔE between each ion and a water molecule, as a function of the $\text{As}\cdots\text{O}_w$ and $\text{B}\cdots\text{O}_w$ distances, with two orientations of water (Figure 6). The first orientation (protons pointing to the

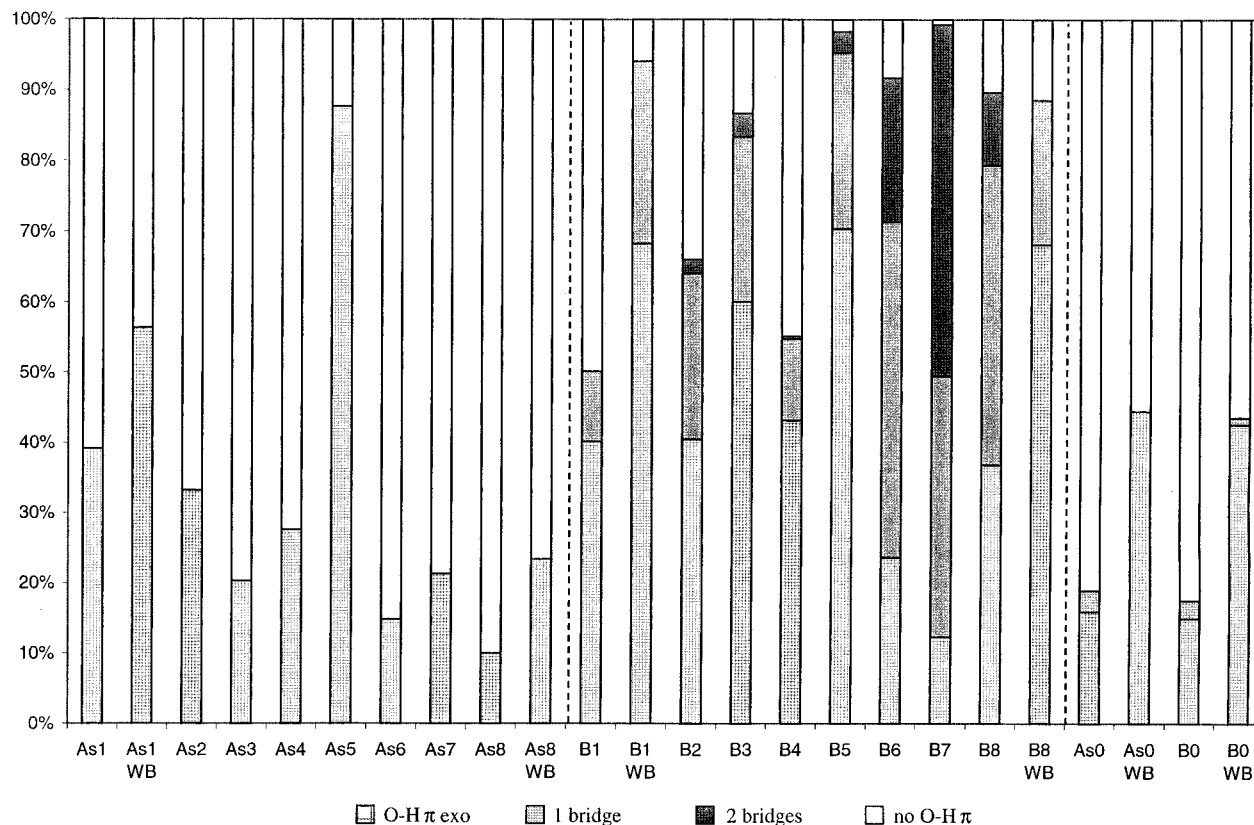


Figure 5. AsPh_4^+ , BPh_4^- ions and AsPh_4^0 , BPh_4^0 simulated in TIP3P water with *set1* to *set8*. Statistical analysis of $\text{OH}-\pi$ interactions: single (*exo*), one bridging water, two bridging waters (see Figure 4). The WB results are obtained with the polarizable model of Wallqvist and Berne.¹⁸

TABLE 2: Ion...Water Supermolecule: Interaction Energy (kcal/mol) between the Ion and H_2O Calculated by MM with Different Charge Distributions and *ab Initio* with Different Basis Sets^a

basis set	AMBER ^b						GAUSSIAN ^c
	ESP	MK-ESP	CHELP	CHELPG	Mulliken	Handmade	
$\Delta E(\text{AsPh}_4^+)$							
3-21G*	-2.7 (<i>set1</i>)	-2.3	-0.8	-1.6	-7.4	3.6 (<i>set6</i>)	1.84
6-311G*		-1.3 (<i>set2</i>)	-0.2	-1.4 (<i>set4</i>)	-6.9 (<i>set5</i>)	4.8 (<i>set7</i>)	2.61
6-311G(df,p)		-1.7	-0.4 (<i>set3</i>)	-0.7	-4.3	2.4 (<i>set8</i>)	2.64
$\Delta E(\text{BPh}_4^-)$							
3-21G*	-12.3 (<i>set1</i>)	-11.8	-9.4	-10.5	-15.8	-8.5 (<i>set6</i>)	-8.38
6-311G*		-11.5 (<i>set2</i>)	-8.7	-9.7 (<i>set4</i>)	-15.6 (<i>set5</i>)	-9.7 (<i>set7</i>)	-7.46
6-311G(df,p)		-10.7	-8.4 (<i>set3</i>)	-9.5	-13.1	-7.5 (<i>set8</i>)	-6.67

^a The $\text{B}\cdots\text{O}$ and $\text{As}\cdots\text{O}$ distances are fixed at 4.6 Å (the bridging structure is shown in Figure 4, middle). ^b Molecular mechanical results. ^c Quantum mechanical results with BSSE correction.

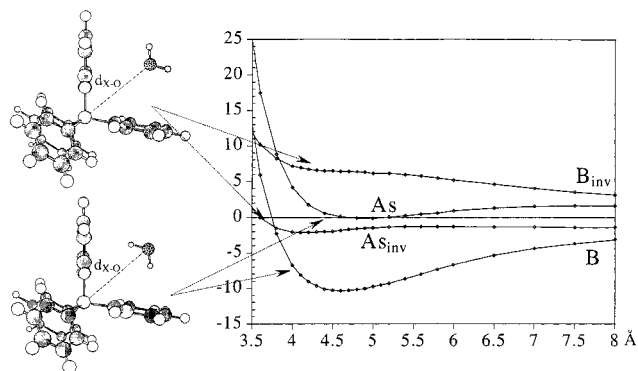


Figure 6. Interaction energy (kcal/mol) among AsPh_4^+ , BPh_4^- , and H_2O , with two orientations of the water dipole (3-21G* basis set).

ion) allows for bridging $\text{OH}\cdots\pi$ contacts. The corresponding energy curve shows a flat energy minimum for BPh_4^- of about -10 kcal/mol at a $\text{B}\cdots\text{O}_w$ distance of 4.5–4.7 Å, while at similar distances ΔE is nearly zero for AsPh_4^+ . The second orientation of water is inverted (the oxygen atom points to the

ion) and yields repulsive interactions with BPh_4^- at all distances, and small attractions (about 1 kcal/mol) with AsPh_4^+ between 4 and 8 Å (Figure 6).

The interaction energy ΔE of bridging water with the ions was recalculated in the $\text{AsPh}_4^+\cdots\text{H}_2\text{O}$ and $\text{BPh}_4^-\cdots\text{H}_2\text{O}$ supermolecules (rigid geometry), forming a π bridging arrangement, at $\text{As}\cdots\text{O}_w$ and $\text{B}\cdots\text{O}_w$ distances of 4.6 Å (see Figure 4, middle), using different methods. The resulting BSSE corrected ΔE values are reported in Table 2, from *ab initio* calculations using the 3-21G*, 6-311G*, and 6-311G(df,p) basis sets, and from molecular mechanics calculations with *set1* to *set8*. The *ab initio* results confirm that bridging solvation is attractive for BPh_4^- (ΔE ranges from -6.7 to -8.4 kcal/mol), but slightly repulsive for AsPh_4^+ (ΔE ranges from 1.8 to 2.6 kcal/mol).

The *ab initio* results may be used as a reference to assess the performance of *set1* to *set8*. All sets correctly yield attractive water interactions with BPh_4^- . The *set5* (Mulliken) values (-15 kcal/mol) are clearly exaggerated. As noted above, the choice of basis set has less effect on ΔE than the fitting procedure, and ΔE is more attractive with ESP (*set1*) and MK-

TABLE 3: AsPh_4^+ and BPh_4^- Species Simulated in TIP3P Water and Chloroform Solutions with the RF Correction: Average Solute–Solvent Interaction Energies E_{sx} and their Electrostatic $E_{\text{sx,elec}}$ and van der Waals $E_{\text{sx,vdw}}$ Components (kcal/mol)^a

		Water									
		<i>set1</i>	<i>set1</i> WB	<i>set2</i>	<i>set3</i>	<i>set4</i>	<i>set5</i>	<i>set6</i>	<i>set7</i>	<i>set8</i>	<i>set8</i> WB
AsPh_4^+											
$E_{\text{sx,vdw}}$		−31.9	−68.2	−31.7	−32.3	−32.3	−27.5	−33.5	−31.8	−33.3	−69.5
$E_{\text{sx,elec}}$		−33.0	−28.2	−35.3	−29.4	−29.5	−67.7	−43.7	−65.0	−34.5	−28.0
E_{sx}		−64.9	−96.8	−67.0	−61.8	−61.8	−95.2	−77.1	−96.8	−67.8	−97.6
BPh_4^-											
$E_{\text{sx,vdw}}$		−27.7	−65.9	−27.7	−29.9	−29.1	−23.4	−31.0	−29.7	−30.3	−68.6
$E_{\text{sx,elec}}$		−109.9	−76.8	−103.8	−67.6	−79.0	−157.5	−68.8	−92.6	−57.1	−48.0
E_{sx}		−137.6	−142.8	−131.4	−97.5	−108.0	−180.9	−99.8	−122.3	−87.4	−114.7
		Chloroform									
		<i>set1</i>	<i>set2</i>	<i>set3</i>	<i>set4</i>	<i>set5</i>	<i>set6</i>	<i>set7</i>	<i>set8</i>		
AsPh_4^+											
$E_{\text{sx,vdw}}$		−46.9	−45.1	−45.8	−46.2	−48.2	−46.4	−47.9	−46.5		
$E_{\text{sx,elec}}$		−21.1	−22.8	−21.7	−22.2	−20.0	−24.3	−24.5	−24.6		
E_{sx}		−68.0	−67.9	−67.5	−68.4	−68.2	−70.7	−73.2	−71.3		
BPh_4^-											
$E_{\text{sx,vdw}}$		−48.1	−46.7	−47.9	−47.6	−48.7	−47.9	−48.1	−47.5		
$E_{\text{sx,elec}}$		−32.7	−29.8	−27.6	−29.3	−39.5	−28.1	−30.3	−25.3		
E_{sx}		−80.8	−76.5	−75.5	−76.9	−88.3	−75.9	−78.4	−72.8		

^a Fluctuations are about 5 kcal/mol. The WB results are obtained with the polarizable model.¹⁸

ESP (*set2*) models than with CHELP (*set3*) and CHELPG (*set4*) models. Concerning the $\text{AsPh}_4^+\cdots\text{H}_2\text{O}$ interactions, agreement between force field and QM results is less good, as ΔE is repulsive with the ab initio calculations (1.8–2.6 kcal/mol), as well as with the *set6* to *set8* charges (2.4–4.8 kcal/mol), but attractive with the QM derived charges of *set1* to *set5*. The largest deviation is again found with the Mulliken charges (ΔE ranges from −4.3 to −7.3 kcal/mol). Surprisingly, the best agreement with both BPh_4^- and AsPh_4^+ is obtained with the handmade *set8* model, where the charge is equally spread on all atoms (Table 2). Whether *set8* also best describes other solvent configurations is unclear and requires additional investigations. This is why we consistently compare *set1* to *set8* representations of the ions in the following.

Interaction Energies of AsPh_4^+ and BPh_4^- with the Solvents, as a Function of the Charge Distribution. The total solute–solvent interaction energies E_{sx} and their electrostatic $E_{\text{sx,elec}}$ and van der Waals $E_{\text{sx,vdw}}$ components, calculated in TIP3P water and OPLS chloroform, are reported in Table 3. The E_{sx} energies are model dependent. However, in both solvents and with all eight models, the anion displays larger attractions than the cation with the solvent.

In aqueous solution, the difference ΔE_{sx} stems mostly from the difference $\Delta E_{\text{sx,elec}}$ in electrostatic contributions, which ranges from 39 to 90 kcal/mol (*set1* to *set5* QM models) and from 23 to 28 kcal/mol (*set6* to *set8* models). Again, the Mulliken charges (*set5*) give the largest ion differentiation (90 kcal/mol), due to exaggerated interactions of the anion with water. The van der Waals $E_{\text{sx,vdw}}$ component is nearly model independent, and about 2 kcal/mol more attractive for AsPh_4^+ than for BPh_4^- . These contributions are nearly the same in the ions as in the AsPh_4^0 and BPh_4^0 all-neutral species (−32.3 and −30.7 kcal/mol, respectively). The anion also interacts better than the cation with the WB water model, by 17 kcal/mol (*set8* charges) and 46 kcal/mol (*set1* charges).

In chloroform solution, electrostatic interactions are weaker than in water, while van der Waals attractions are larger. The differences in E_{sx} energies of AsPh_4^+ vs BPh_4^- are smaller (1–20 kcal/mol) than in water and are again the largest with *set5*. The anion solvation is (slightly) favored by both electrostatic and van der Waals components.²⁸ In water, the *set8* model which

best fits the ab initio results of the ion–water dimer yields the smallest, although still significant, difference in interaction energies with water ($\Delta E_{\text{sx}} = 20$ kcal/mol), while in chloroform the corresponding difference is 1 kcal/mol only.

Differences in Free Energies of Solvation of AsPh_4^+ and BPh_4^- in Water and Chloroform Solutions, as a Function of the Charge Distribution. The difference in free energies of solvation between AsPh_4^+ and BPh_4^- can be calculated stepwise as $\Delta G^{+-} = \Delta G^{+0} + \Delta G^{00} + \Delta G^{0-}$, using the definitions given in eqs 2–5. The results obtained with the corrected RF method are given in Table 4.

We first notice that the ΔG^{00} energy, which corresponds to the solvation energy difference between the all-neutral AsPh_4^0 and BPh_4^0 species, is small (−0.4 kcal/mol in water and −0.1 kcal/mol in chloroform) and negative, as suggested by the Born model and the somewhat smaller size of BPh_4^0 . Thus, differences in solvation energies are determined by the changes in free energies of ion charging ΔG^{0+} and ΔG^{0-} . With all models this process is favorable ($\Delta G < 0$), and more favorable in water than in chloroform. Most important is the difference in cation vs anion solvation energies.

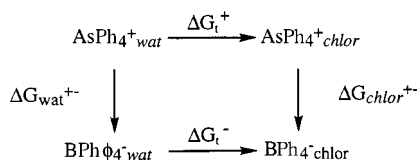
Table 4 shows that, in water, all sets of charges yield the same conclusion: the BPh_4^- anion is better hydrated than AsPh_4^+ , by about 20–44 kcal/mol. The three handmade models yield similar ΔG^{+-} values (−21 to −23 kcal/mol), close to those obtained with *set3* (−27 kcal/mol), while Mulliken charges give intermediate values (−32 kcal/mol).

The results obtained with the TIP3P water model are confirmed with the polarizable WB model, tested with the *set1* and *set8* charges: ΔG^{+-} is −32.5 and −18.2 kcal/mol, respectively, which is somewhat less negative than with the TIP3P water, but still indicates a marked preference for the anion’s hydration.

In OPLS chloroform solution, the ΔG^{+-} energies are smaller than in water and model dependent. No firm conclusion can be drawn as ΔG^{+-} ranges from positive to negative values (+4.2 to −4.5 kcal/mol). ΔG^{+-} is positive with the handmade models and with *set3* (1.5–4.2 kcal/mol), while QM derived models yield either positive or negative ΔG^{+-} values. Using the all-atom polarizable model of chloroform in conjunction with the most delocalized (*set8*) charges yields a better solvation of the cation ($\Delta G^{+-} = 12.3$ kcal/mol).

TABLE 4: Free Energy Results (kcal/mol) in Pure Water and Chloroform Obtained with the RF Corrected Treatment of Electrostatics

Solvent		$-\Delta G_s^{0+}$	ΔG_s^{00}	$-\Delta G_s^{0-}$	ΔG_s^{+-}	$\Delta \Delta G_t^{a)}$
		$\text{AsPh}_4^+ \longrightarrow \text{AsPh}_4^0$	$\longrightarrow \text{BPh}_4^0$	$\longrightarrow \text{BPh}_4^-$		
TIP3P Water	<i>set 1</i>	8.0	-0.4	-51.9	-44.3	-
	<i>set 2</i>	8.0	-0.4	-50.0	-42.4	-
	<i>set 3</i>	6.1	-0.4	-32.3	-26.6	-
	<i>set 4</i>	6.4	-0.4	-37.7	-31.7	-
	<i>set 5</i>	46.1	-0.4	-77.0	-31.3	-
	<i>set 6</i>	12.1	-0.4	-34.1	-22.4	-
	<i>set 7</i>	20.1	-0.4	-42.3	-22.6	-
	<i>set 8</i>	7.9	-0.4	-28.7	-21.2	-
WB Water + pol	<i>set 1</i>	4.8	-0.4	-37.5	-32.5	-
	<i>set 8</i>	8.8	-0.4	-26.6	-18.2	-
OPLS Chloroform	<i>set 1</i>	9.3	-0.1	-13.3	-4.1	-40.2
	<i>set 2</i>	10.4	-0.1	-10.8	-0.5	-41.9
	<i>set 3</i>	11.1	-0.1	-6.8	4.2	-30.8
	<i>set 4</i>	9.9	-0.1	-9.6	0.3	-32.0
	<i>set 5</i>	10.0	-0.1	-14.8	-4.5	-26.8
	<i>set 6</i>	11.2	-0.1	-8.5	2.6	-25.0
	<i>set 7</i>	12.3	-0.1	-10.7	1.5	-24.1
	<i>set 8</i>	11.7	-0.1	-8.1	3.5	-24.7
5 pts Chloroform + pol	<i>set8</i>	11.6	-0.1	0.8	12.3	-30.5

SCHEME 1

With the standard calculations (Table S1), the ΔG^{0+} values are too large, while the ΔG^{0-} ones are too weak, due to artifacts in the treatment of boundaries.¹² Thus, as noticed for spherical solutes,¹² the ΔG^{+-} results obtained with the standard cutoff lead to conclusions opposite those obtained with the RF method.

Differences in Free Energies of Transfer of AsPh_4^+ vs BPh_4^- Ions from TIP3P Water to OPLS Chloroform, as a Function of the Charge Distribution. The difference in free energies of transfer of AsPh_4^+ vs BPh_4^- from water to another solvent can be, in principle, assessed by computations, using the thermodynamic cycle shown in Scheme 1. According to this cycle, the difference $\Delta \Delta G_t$ between the free energies of transfer ΔG_t^+ of the cation and ΔG_t^- of the anion can be obtained by $\Delta \Delta G_t = \Delta G_t^+ - \Delta G_t^- = \Delta G_{\text{wat}^{+-}} - \Delta G_{\text{chlor}^{+-}}$.

The $\Delta G_{\text{wat}^{+-}}$ and $\Delta G_{\text{chlor}^{+-}}$ energies have been reported above in pure solvent phases.

Combining the $\Delta G_{\text{wat}^{+-}}$ and $\Delta G_{\text{chlor}^{+-}}$ energies leads to a difference ΔG_t^{+-} in free energies of transfer. The values reported in Table 4 yield the same conclusions with all sets of charges, with the two water models: *the AsPh_4^+ cation is more easily transferred than BPh_4^- from water to chloroform.* This is observed with the standard TIP3P and OPLS solvent models, as well as with the polarizable WB water and Chang and Dang chloroform models. As *set1* charges on the ions somewhat overestimate the anion affinity for water, the corresponding value of $\Delta \Delta G_t$ (-40.2 kcal/mol) is likely exaggerated. It remains, however, that the smallest calculated value of $\Delta \Delta G_t$ is still quite large (-24.1 kcal/mol).

Again, using standard treatment of the boundaries instead of the RF correction yields the inverse conclusion (Table S1).

Discussion and Conclusion

MD and FEP simulations on model tetrahedral AsPh_4^+ and BPh_4^- hydrophobic ions, using eight different charge distributions, show that *sign reversal of the ionic charge leads to marked differences in solvation properties in pure water and chloroform solutions.* The largest sign discrimination is found in water, where BPh_4^- is better hydrated than AsPh_4^+ . This is found with two water representations: the widely used TIP3P model and the polarizable WB model. The conclusions obtained with the tetrahedral ions are qualitatively similar to those obtained with large hydrophobic spherical ones.¹² According to the simulations, the preferred hydration of the anion stems from two main features. First, the AsPh_4^0 and BPh_4^0 all-neutral species are “electrostatically preorganized” for anion charging, as the electrostatic potential ϕ at their center is positive (about 8.0 kcal/mol) with both TIP3P and WB water models and 11 Å + RF as well as PME Ewald calculations.²⁹ Second, the anion displays, with both water models, specific hydration patterns (OH- π interactions). Thus, the effect of charge reversal cannot be simply assessed by solvent continuum models.

There are many factors that contribute to the solvation thermodynamics of ions, and the effect of sign inversion is unclear.³⁰ Discussions on computational aspects can be found in refs 31–39. Our conclusion obtained with corrected treatment of the boundaries is consistent with previous theoretical results. Using polarizable Langevin dipoles or explicit solvent molecules,⁴⁰ Luzhkov and Warshel concluded that BPh_4^- is better hydrated than PPh_4^+ , due to the differences in charge distribution and to “steric factors”. In the case of small spherical ions (e.g., Cl^-/Cl^+), RISM-HNC calculations also suggest that cations are less hydrated than anions, due to differences in their “effective size”.³¹ Hummer et al. also calculated “negative ions to be solvated more strongly, compared to positive ions of equal size”.³⁸ Lynden-Bell and Rasaiah simulated ions in SPC/E water and presented “direct evidence of the asymmetry in the free energy, enthalpy and entropy of hydration of ions on charge inversion arising from the asymmetry in the charge distribution

in a water molecule^{37,41} Charge inversion also modifies dynamics features, as the fictitious I^+ cation was calculated to be less mobile than the iodide I^- anion in water.⁴²

Combining the results obtained in the two solvents leads to the important conclusion that *AsPh₄⁺ is more easily transferred than BPh₄⁻ from water to chloroform*. This is trend is the same as for the spherical S^+ and S^- isosteric analogues.¹² For the latter, we showed that RF results were nearly identical to those obtained with Ewald and different integration schemes (thermodynamic integration vs windowing FEP). The results are in contradiction with the TATB assumption, but qualitatively consistent with electrochemical measurements by Girault et al., who found that AsPh_4^+ is more easily transferred than BPh_4^- from water to 1,2-dichloroethane across the interface (the corresponding standard Gibbs energies are -9.6 and -8.6 kcal/mol, respectively).⁴³ We notice that, in the latter case, the organic solvent is different from chloroform and may not be dry.

The marked difference in calculated hydration patterns of the two tetrahedral ions is also consistent with a number of experimental results in the solid state and in solution. We analyzed the hydration of AsPh_4^+ and BPh_4^- in solid-state structures retrieved from the Cambridge crystallographic structural database.²⁴ In no case was water bound to AsPh_4^+ , while several examples of bridging water, identical to the simulated ones, were found for BPh_4^- . Structures are reported in ref 44. In the aqueous solution, spectroscopy studies of the HDO water molecules surrounding BPh_4^- and the PPh_4^+ analogue of AsPh_4^+ revealed distinct differences in their hydration. They concluded that the anion interacts more with water than the cation and that “the effect of BPh_4^- is determined by the anion–water interactions, while the effect of PPh_4^+ is determined by water–water interactions around the cation”.⁴⁵

Our results are quite disturbing in the context of the “TATB hypothesis”, as we calculate that the ions display *marked differences of solvation properties, which depend on the sign of the ionic charge and on the nature and hydrogen-bonding capabilities of the solvent*.

On the computational side, we previously addressed a number of issues concerning the treatment of boundaries, “long-range electrostatics”, and the energy representation of the systems.^{6,12} The cutoff value of 11 Å used here in water may seem small, but is not critical, as using a larger cutoff (15 Å) led to nearly identical ΔG^{+-} differences in free energies of solvation of S^+ vs S^- analogues.¹² Other simulations in chloroform also gave identical values with 15 and 20 Å cutoffs.⁶ The treatment of boundaries is crucial, as standard calculations using a residue-based cutoff led to artifacts and conclusions opposite those obtained with corrected treatments. Another issue concerns the choice of atomic charges on the ions, which stimulated this study. Although many other choices of atomic charges can be repeatedly tested (see for instance refs 46–48), we believe that there is no major artifact, as the eight very different sets tested lead to the same qualitative conclusion concerning the preferred anion hydration, and to reasonable interactions within the ion–water supermolecules. According to the TATB hypothesis, the details of charge distribution should not be so crucial. However, we find energy differences of up to 20 kcal/mol for ΔG^{+-} in TIP3P water, as a function of the charge distribution. In WB water, the value of ΔG^{+-} is comparable (18.2 kcal/mol with *set8*). It seems unlikely that some other choice of charges would lead to identical solvation energies of the cation and the anion.

Other critical parameters may concern the solvent. The ones we used were derived from pure liquid-phase properties, and may not accurately describe their mutual competition with the

solutes, or their interactions with hydrophobic species. Explicit representation of nonadditivity and polarization effects may be crucial in the context of the TATB hypothesis, as shown for ions in chloroform^{19,49} and in water,^{20,49–51} as well as for hydrophobic interactions in water.^{49,52,53} Classical water models hardly account for the dielectric properties of water (see for instance re 54) and may be too polar to depict aqueous interfaces.⁵⁵ We previously compared the solvation of S^+ and S^- spheres with Chang’s polarized models of water⁵⁶ and of chloroform¹⁹ and came to the same conclusions as with the unpolarized ones.¹² Here, the comparison of the TIP3P with the polarizable WB model, which accounts for the dipole moment of the H_2O in the gas phase and in solution, leads to the same conclusions: two consistently derived models of AsPh_4^+ and BPh_4^- are found to interact very differently with a given model of solvent, and the anion is better hydrated than the cation. Whether other solvent models (e.g., recently developed TIP5P⁵⁷ or Guillot models)⁵⁸ lead to identical free energies of solvation and of transfer from water to another solvent remains to be investigated.

Another possible source of \pm ion discrimination relates to the “humidity” of the organic phase. We feel that some care should be taken concerning the interpretation of experiments. On the basis of partition coefficients, Osakai et al. concluded that no water is extracted with such ions to nitrobenzene, which is more polar than chloroform.⁵⁹ However, according to computer simulations⁶ and to NMR⁶⁰ and conductivity measurements on related systems,⁶¹ such ions form intimate ion pairs or aggregates, which should display less affinity for water than the “naked” ions, transferred in electrochemical experiments.⁴³ Our simulations in pure water, as well as in wet chloroform solutions⁶² indicate that the naked anion interacts more than the naked cation with water. Considering a $\text{BPh}_4^-, n\text{H}_2\text{O}$ supermolecule in the organic phase thus may contribute to the reduction in the difference in free energies of transfer between the anion and the cation, it is not enough, however, to compensate for the difference of more than 20 kcal/mol in free energies of transfer.

Our study should stimulate further theoretical treatments with a particular focus on polarization and nonadditivity effects, as well as experiments on the effect of the charge of ions and properties in solution. The TATB problem represents a challenging test for other solvent models. Fundamentally, our results have bearing on our understanding of the hydrophilic/hydrophobic character of neutral and large ionic solutes and on their behavior at aqueous interfaces as well as in heterogeneous environments. One important question concerns the solution state of such hydrophobic ions. As the $\text{AsPh}_4\text{BPh}_4$ salt has a very low solubility in water (about $10^{-8.5}$ mol/L),² AsPh_4^+ and BPh_4^- are generally studied with more hydrophilic counterions, whose role remains to be investigated. Another issue relates to the surfactant behavior of AsPh_4^+ and BPh_4^- , revealed by simulations^{6,63} and experiment.⁶⁴ As surfactants may form in solution supramolecular assemblies which may range from aggregates to micelles, it remains to be assessed whether the solutions where experimental studies on the TATB assumption have been carried out can be modeled by pure homogeneous solutions as those simulated here.

Acknowledgment. We are grateful to IDRIS and the Université Louis Pasteur for computer resources and to PRACTIS for support. R.S. thanks the French Ministry of Research for a grant.

Supporting Information Available: Table listing the free energy results in pure water and chloroform obtained with the standard and RF-corrected treatments of electrostatics and figures showing the angles around the As–Ph and B–Ph bonds as a function of time from simulations in water with *set1*, *set4*, and *set5* and AsPh₄⁺ and BPh₄[−] ions in chloroform simulated with different charge distributions. This material is available free of charge via the Internet at <http://pubs.acs.org>.

References and Notes

- (1) Grunwald, E.; Baughman, G.; Kohnstam, G. *J. Am. Chem. Soc.* **1960**, *82*, 5801–5811.
- (2) Kim, J. I. *J. Phys. Chem.* **1978**, *82*, 191–199.
- (3) Marcus, Y. *Ion Solvation*; Wiley: Chichester, 1985.
- (4) Born, M. *Z. Phys.* **1920**, *1*, 45. For a recent discussion, see Ashbaugh, H. S. *J. Phys. Chem. B* **2000**, *104*, 7235–7238.
- (5) Marcus, Y. *Pure Appl. Chem.* **1987**, *9*, 1093–1101. Kalidas, C.; Hefter, G.; Marcus, Y. *Chem. Rev.* **2000**, *100*(3), 820–839 and references cited therein.
- (6) Schurhammer, R.; Wipff, G. *New J. Chem.* **1999**, *23*, 381–391.
- (7) Ashbaugh, H. S.; Sakane, S.; Wood, R. H. *J. Phys. Chem. B* **1998**, *102*, 3844–3845 and references therein.
- (8) Madura, J. D.; Pettitt, B. M. *Chem. Phys. Lett.* **1988**, *150*, 105–108.
- (9) Hummer, G.; Pratt, L. R.; Garcia, A. E.; Garde, S.; Berne, B. J.; Rick, S. W. *J. Phys. Chem. B* **1998**, *102*, 3841–3843 and references therein.
- (10) Åqvist, J.; Hansson, T. *J. Phys. Chem. B* **1998**, *102*, 3837–3840 and references therein.
- (11) Ashbaugh, H. S.; Wood, R. H. *J. Chem. Phys.* **1997**, *106*, 8135–8139.
- (12) Schurhammer, R.; Wipff, G. *J. Mol. Struct.: THEOCHEM* **2000**, *500/123*, 139–155.
- (13) Case, D. A.; Pearlman, D. A.; Caldwell, J. C.; Cheatham, T. E., III; Ross, W. S.; Simmerling, C. L.; Darden, T. A.; Merz, K. M.; Stanton, R. V.; Cheng, A. L.; Vincent, J. J.; Crowley, M.; Ferguson, D. M.; Radmer, R. J.; Seibel, G. L.; Singh, U. C.; Weiner, P. K.; Kollman, P. A. AMBER5, University of California, San Francisco, 1997.
- (14) Cornell, W. D.; Cieplak, P.; Bayly, C. I.; Gould, I. R.; Merz, K. M.; Ferguson, D. M.; Spellmeyer, D. C.; Fox, T.; Caldwell, J. W.; Kollman, P. A. *J. Am. Chem. Soc.* **1995**, *117*, 5179–5197.
- (15) In BPh₄[−] and AsPh₄⁺, rotation of one phenyl group is somewhat hindered by the three others (gearing effect). According to MD simulations of 200 ps on the gas phase, there is no rotation for BPh₄[−] nor BPh₄⁰ (all-neutral model), while AsPh₄⁺ and AsPh₄⁰ (all-neutral model) display several rotations, as in solution. Conversely, simulating BPh₄[−] with longer bonds (1.91 Å) leads to rotation, while AsPh₄⁺ simulated with shorter bonds (1.66 Å) does not rotate. Thus, with our force field parameters, internal rotation is mainly controlled by the As–C vs B–C distance, and not determined by solvation effects.
- (16) Jorgensen, W. L.; Chandrasekhar, J.; Madura, J. D. *J. Chem. Phys.* **1983**, *79*, 926–936.
- (17) Jorgensen, W. L.; Briggs, J. M.; Contreras, M. L. *J. Phys. Chem.* **1990**, *94*, 1683–1686.
- (18) Wallqvist, A.; Berne, B. J. *J. Chem. Phys.* **1993**, *97*, 13841–13851.
- (19) Chang, T.-M.; Dang, L. X.; Peterson, K. A. *J. Phys. Chem. B* **1997**, *101*, 3413–3419.
- (20) Dang, L. X.; Rice, J. E.; Caldwell, J.; Kollman, P. A. *J. Am. Chem. Soc.* **1991**, *113*, 2481–2486.
- (21) Smith, P. E.; van Gunsteren, W. F. In *Computer Simulations of Biomolecular Systems*; van Gunsteren, W. F., Weiner, P. K., Wilkinson, A. J., Eds.; ESCOM: Leiden, 1993; pp 182–212.
- (22) Tironi, I. G.; Sperber, R.; Smith, P. E.; van Gunsteren, W. F. *J. Chem. Phys.* **1995**, *102*, 5451–5459.
- (23) Frisch, M. J.; Trucks, G. W.; Schlegel, H. B.; Gill, P. M. W.; Johnson, B. G.; Robb, M. A.; Cheeseman, J. R.; Keith, T.; Petersson, G. A.; Montgomery, J. A.; Raghavachari, K.; Al-Laham, M. A.; Zakrzewski, V. G.; Ortiz, J. V.; Foresman, J. B.; Peng, C. Y.; Ayala, P. Y.; Chen, W.; Wong, M. W.; Andres, J. L.; Replogle, E. S.; Gomperts, R.; Martin, R. L.; Fox, D. J.; Binkley, J. S.; Defrees, D. J.; Baker, J.; Stewart, J. P.; Head-Gordon, M.; Gonzales, C.; Pople, J. A. *Gaussian 94*, Revision B.2.; Gaussian, Inc.: Pittsburgh, PA, 1995.
- (24) Allen, F. H.; Kennard, O. *Chem. Des. Autom. News* **1993**, *8*, 31–37.
- (25) Wavefunction Inc., Irvine, CA, 1995.
- (26) Engler, E.; Wipff, G. In *Crystallography of Supramolecular Compounds*; Tsoucaris, G., Ed.; Kluwer: Dordrecht, The Netherlands, 1996; pp 471–476.
- (27) This is supported by simulations on AsPh₄⁺ in water with “short bonds” (using the B–C distances), which does not lead to internal rotation, but to the same hydrogen-bonding patterns as with “real bonds”. Similarly, BPh₄[−] simulated with “long” B–C bonds (As–C distances) displays nearly identical hydration patterns as with “real” bond distances.
- (28) This corresponds to different solvation patterns of the anion, compared to the cation. According to the RDFs (Figure S2) all models yield similar patterns of a given ion. AsPh₄⁺ makes closer contacts with Cl_{chlor} than with H_{chlor}, while H_{chlor} points to the center of BPh₄[−].
- (29) These potential values are close to those calculated for the neutral sphere S⁰ in water (about 10 kcal/mol) with the RF method as used here, the PME Ewald method, as well as the M3 residue-based method. As discussed in refs 7–12 there is general consensus on this value of the potential. In chloroform, the potential at neutral tetrahedral AsPh₄⁰ and BPh₄⁰ solutes is negative (−4.5 kcal/mol) and also close to the value for S⁰ (−5.0 kcal/mol).
- (30) Parker, A. J.; Alexander, R. *J. Am. Chem. Soc.* **1968**, *90*, 3313–3319.
- (31) Roux, B.; Yu, H.-A.; Karplus, M. *J. Phys. Chem.* **1990**, *94*, 4683–4688.
- (32) Schaefer, M.; Karplus, M. *J. Phys. Chem.* **1996**, *100*, 1578–1599.
- (33) Warshel, A.; Russell, S. T. *Q. Rev. Biophys.* **1984**, *17*, 283–422.
- (34) Rashin, A. A.; Honig, B. *J. Phys. Chem.* **1985**, *89*, 5588–5593.
- (35) Maroncelli, M. *J. Chem. Phys.* **1991**, *94*, 2084–2103.
- (36) Åqvist, J.; Hansson, T. *J. Phys. Chem.* **1996**, *100*, 9512–9521.
- (37) Babu, C. S.; Lim, C. *J. Phys. Chem. B* **1999**, *103*, 7958–7968.
- (38) Hummer, G.; Pratt, L. R.; Garcia, A. E. *J. Phys. Chem.* **1996**, *100*, 1206–1215.
- (39) Hummer, G.; Pratt, L. R.; Garcia, A. E. *J. Phys. Chem. A* **1998**, *102*, 7885–7895.
- (40) Luzhkov, V.; Warshel, A. *J. Comput. Chem.* **1992**, *13*, 199–213.
- (41) Lynden-Bell, R. M.; Rasaiah, J. C. *J. Chem. Phys.* **1997**, *107*, 1981–1991.
- (42) Koneshan, S.; Rasaiah, J. C.; Lyden-Bell, R. M.; Lee, S. H. *J. Phys. Chem. B* **1998**, *102*, 4193–4204.
- (43) Shao, Y.; Stewart, A. A.; Girault, H. H. *J. Chem. Soc., Faraday Trans.* **1991**, *87*, 2593–2597.
- (44) Bakshi, P. K. *Can. J. Chem.* **1994**, *72*, 1273.
- (45) Stangret, J.; Kamińska-Piotrowicz, E. *J. Chem. Soc., Faraday Trans.* **1997**, *93*, 3463–3466.
- (46) Sigfridsson, E.; Ryde, U. *J. Comput. Chem.* **1998**, *19*, 377–395.
- (47) Gogonea, V.; Merz, K. M. *J. Phys. Chem. B* **2000**, *104*, 2117–2122.
- (48) Li, J.; Zhu, T.; Cramer, C. J.; Truhlar, D. G. *J. Chem. Phys.* **1998**, *109*, 1820–1831.
- (49) New, M. H.; Berne, B. J. *J. Am. Chem. Soc.* **1995**, *117*, 7172–7179.
- (50) Dang, L. X. *J. Chem. Phys.* **1992**, *97*, 2659–2660.
- (51) Soetens, J.-C.; Millot, C.; Chipot, C.; Jansen, G.; Angyan, J. G.; Maigret, B. *J. Phys. Chem. B* **1997**, *101*, 10910–10917.
- (52) Chang, T.-M.; Peterson, K. A.; Dang, L. X. *J. Chem. Phys.* **1995**, *103*, 7502–7513.
- (53) Young, W. S.; Brooks, C. L., III. *J. Phys. Chem.* **1997**, *106*, 9265–9270.
- (54) Soetens, J.-C.; Martins Costa, M. T. C.; Millot, C. *Mol. Phys.* **1998**, *94*, 577–579 and references therein.
- (55) Sokhan, V. P.; Tildesley, D. J. *Faraday Discuss.* **1996**, *104*, 193–208.
- (56) Chang, T. M.; Dang, L. X. *J. Chem. Phys.* **1996**, *104*, 6772–6783.
- (57) Mahoney, M. W.; Jorgensen, W. L. *J. Chem. Phys.* **2000**, *112*, 8910–8922.
- (58) Guillot, B.; Guissani, Y. In *Steam, Water and Hydrothermal Systems. Physics and Chemistry Meeting the Needs of Industry*; Trentaine, P. R., Hill, P. G., Irish, D. E., Balakrishnan, P. V., Eds.; NRC Research Press: Ottawa, 2000; p 562.
- (59) Osakai, T.; Ogata, A.; Ebina, K. *J. Phys. Chem. B* **1997**, *101*, 8341–8348.
- (60) Dupont, J.; Suarez, P. A. Z.; de Souza, R. F.; Burrow, R. A.; Kintzinger, J.-P. *Chem. Eur. J.* **2000**, *6*, 2377–2381.
- (61) Victor, P. J.; Muhuri, P. K.; Das, B.; Hazra, D. K. *J. Phys. Chem. B* **1999**, *103*, 11227–11232.
- (62) To investigate this issue, we simulated the AsPh₄⁺·4H₂O and BPh₄[−]·4H₂O “supermolecules” in OPLS chloroform for 200 ps, starting with bridging water arrangements (with *set1* and *set8* ion charges). The four water molecules rapidly dissociated from the cation to form water dimers or monomers. This contrasts with BPh₄[−], which remained hydrated by the four H₂O molecules (*set1* charges) or one to two H₂O molecules (*set8* charges). Thus, ΔG⁰⁺ should be similar in “wet” and in dry chloroform, while ΔG^{0−} should be somewhat larger in wet chloroform. According to FEP simulations on the BPh₄[−]·4H₂O → BPh₄⁰·4H₂O mutation, ΔG^{0−} is more negative than in dry chloroform (by about 15 kcal/mol with the *set1* charges).
- (63) Berny, F.; Schurhammer, R.; Wipff, G. *Inorg. Chim. Acta* **2000**, *300–302*, 384–394 (Special Issue).
- (64) Conboy, J. C.; Richmond, G. L. *J. Phys. Chem. B* **1997**, *101*, 983–990.